J Seismol (2021) 25:1077–1087
https://doi.org/10.1007/s10950-021-10013-4

ORIGINAL ARTICLE

Revisiting M_L determination in Taiwan based on the expectation-maximization algorithm

Ting-Chung Huang · Yih-Min Wu

Received: 5 March 2021 / Accepted: 10 May 2021 / Published online: 2 June 2021

Abstract The local magnitude scale M_L is defined by the difference between the observed amplitude ($\log A$) and the anchored attenuation amplitude ($\log A_0$). A previous study in Taiwan established a model of the anchored amplitude as a function of the hypocentral distance R by matching the M_L to the corresponding moment magnitude M_W. Although the overall performance of the model is adequate, there remain some drawbacks, namely, the correlated empirical station correction problem and relatively low sample size. In this paper, we adopt the concept of the expectation-maximization (EM) algorithm to develop a new method that can simultaneously estimate the anchored amplitude model coefficients and station corrections. The revised catalog using the latest dataset in Taiwan provides an up-to-date accurate estimate of M_L. Additionally, the proposed method can systematically obtain statistically meaningful results and be applied to datasets of other regions in the future.

Keywords Local magnitude · Ground motion · Statistical method

Article highlights: A new method that can simultaneously estimate attenuation function and station corrections is proposed. Based on the new method, an updated local magnitude has been established. Using amplitude data in Taiwan, the updated local magnitude shows better consistency with the moment magnitude. The station corrections in Taiwan provide an improved assessment of the geological setting on the island.

1 Introduction

The local magnitude M_L was proposed by (Richter 1935) as a way to connect the single station seismogram reading to the overall strength of an earthquake. Due to its straightforward definition, M_L has been widely adopted by many earthquake monitoring agencies. Although M_L tends to suffer from saturation issues due to its frequency dependence measurement, some studies (Kanamori and Jennings 1978; Bormann and Giacomo 2010) suggest that M_L can better capture the near-field radiation energy of seismic waves

Ting-Chung Huang (✉)
Department of Geosciences, National Taiwan University, 1, Sec. 4, Roosevelt Road, Taipei, 106, Taiwan
e-mail: tingchunghuang@gmail.com

Yih-Min Wu
NTU Research Center for Future Earth, National Taiwan University, Taipei 10617, Taiwan
e-mail: drymwu@ntu.edu.tw

Yih-Min Wu
Institute of Earth Sciences, Academia Sinica, 128, Sec. 2, Academia Road, Nangang, Taipei 11529, Taiwan

than other measurements and is a suitable indicator of possible damage.

Originally, M_L was defined by the amplitude measured on a Wood-Anderson torsion seismograph (Richter 1935; Kanamori and Jennings 1978; Kanamori et al. 1999). They employed a zero-magnitude earthquake in southern California as an anchored reference. A zero-magnitude earthquake is defined as an earthquake that produces a 0.001 mm peak Wood-Anderson amplitude at a station that is 100 km from the epicenter. M_L is derived from the difference in the logarithmic amplitude of the seismograph and the reference zero magnitude logarithmic amplitude, that is,

$$M_L = \log A - \log A_0(\Delta), \tag{1}$$

where the amplitude A is measured in millimeters and Δ denotes the epicentral distance in kilometers. The anchored reference requires that $\log A_0(\Delta = 100) = -3$. In the definition of M_L, the $\log A$ term can be derived directly from the seismograms; the reference term $\log A_0$ requires some modeling.

The previous study of M_L in Taiwan (Shin 1993; Wu et al. 2005) extended the definition of M_L by replacing the dependence of the anchor amplitude A_0 from the epicentral distance Δ to hypocentral distance R in kilometeres. They also utilized the observation that there is a linear relationship between M_L and M_W in Taiwan at magnitudes 4 to 6 for shallow earthquakes. They derived both a refined $\log A_0(R)$ attenuation model in terms of R and a new local magnitude M_L that is consistent with M_W. By triangling with another reference magnitude (M_W in this case), they managed to escape the immediate tautology of a new anchor amplitude model and new local magnitude.

To summarize the approach in detail, we consider the definition of $\log A_0$ in terms of the given data,

$$\log A_0 \approx \log A - M_W + S_i, \tag{2}$$

where $\log A$ is the recorded amplitude at the station, M_W is the moment magnitude of the event, and S_i is the station correction that accounts for the effect of the geological setting of station i. In Wu et al. (2005), this correction was assigned empirically based on the geological setting of the station. For every trace in one event, we can derive a $\log A_0$ and pair with the corresponding R. The data pairs of $\log A_0$ and R are utilized to establish a linear model of $\log A_0$ in terms of R:

$$\log A_0(R) = A + B \cdot \log R, \tag{3}$$

where A and B are linear model coefficients to be determined by regression. Note that $\log A_0$ and $\log A_0(R)$ denote different concepts. $\log A_0$ is a number derived from data, while $\log A_0(R)$ is a function of R that estimates $\log A_0$ at a different hypocentral distance. Once the attenuation model $\log A_0(R)$ is defined, they proceeded to calculate the new local magnitude,

$$M_L = \log A - \log A_0(R) + S_i. \tag{4}$$

Although this triangle approach with renewed $\log A_0(R)$ and M_L works well in Taiwan and has been applied to other regions (Ristau et al. 2016; Rhoades et al. 2020), it has several issues. The first issue is the assignment of the station correction S_i. This term was often manually inserted or calculated based on the empirical interstation difference or inverted all together (Di Bona 2016). The station corrections are arguably trivial if they are small enough; however, this case is not valid in Taiwan. According to Wu et al. (2005), the station correction ranges from −0.4 to 0.4 magnitude units in Taiwan, which is far from negligible. In addition, the previous two equations, Eqs. 2 and 3, suggest that the station corrections interact with the linear model coefficients A and B. A change in one equation will cause a change in the other equation. This notion motivates us to seek a way to simultaneously estimate both the station corrections and the attenuation model coefficients. We strive to find a new method that can reasonably disentengle the effects of station correction and attenuation.

The second issue is the small data size used in previous model building. In Wu et al. (2005), the researchers collected 56 events from a network of 79 stations. In past years, there has been a continual increase in the number of events recorded and the number of new stations installed in Taiwan, so it is important to update the $\log A_0$ model with the latest data.

In this paper, we solve these issues using a new approach that simultaneously estimates two groups of parameters with the most up-to-date data available in Taiwan. The key points of this work are presented as follows:

– We describe the proposed method inspired by the expectation-maximization (EM) algorithm (sub-Section 3.2).
– We show the numerical results of the latest model and compare them to those of previous studies (Section 4).
– We discuss the convergence property of the proposed method and its applicability to other datasets, even without the given empirical station corrections (Section 5).

2 Data

The Central Weather Bureau (CWB) provided earthquake catalog data from 1990 to 2018. A total of 156 stations were applied to estimate the station corrections, compared to the 79 stations that appeared in Wu et al. (2005).

We collected shallow earthquakes (depth < 35 km) with a moment magnitude of approximately 4 to 6 within the Global Centroid Moment Tensor (GCMT) catalog and found 523 matched events within the CWB catalog. The total number of records was 62100, compared to the 56 events and 1898 records in Wu et al. (2005). All those events were relocated using a reliable three-dimensional velocity model (Thurber and Eberthart-Phillips 1999; Wu et al. 2003, 2007, 2008, 2009); therefore, we utilized the location information from the relocation as the primary source.

3 Methodology

3.1 The EM algorithm

The EM algorithm was originally designed to conquer the problem of missing data in maximum likelihood estimation (Hartley 1958; Dempster et al. 1977). The algorithm consists of two parts: the E-step and M-step. The E-step calculates the expectation of the log-likelihood with respect to missing data. Missing data are not an unknown random quantity because the expectation assigns an "average" value to them. The M-step indicates that the fittest parameters maximize the expected log-likelihood. With the updated parameter, we can proceed to the second round of the E-step with an updated expectation and then to the M-step for another parameter update. After a few rounds of alternating the E-step and M-step, both the parameters and the missing data will converge to statistically meaningful results (Neal and Hinton 1998). In typical cases (when the underlying distribution obeys exponential family distributions), the converged parameters coincide with the maximum likelihood estimation without missing data. For a collection of modern developments of the EM algorithm, we can consult (McLachlan and Krishnan 2008).

3.2 Iterative regression

Inspired by the EM algorithm, we propose the iterative regression method to disentangle the station corrections from the $\log A_0$ model parameters by reinterpreting station corrections as missing data in EM. In addition to this change, the iterative regression method replaces the likelihood function optimization process with regression because of a significant reduction in computational cost. Except for the two new features, the iterative regression closely follows the EM algorithm. We will now examine the two steps in iterative regression and their correspondence with the EM algorithm.

Station Correction Estimation: This step corresponds to the E-step. We estimate the station correction factor at the $(r+1)$-th iteration using the existing $\log A_0(R)$ model at the (r)th iteration. The station correction of station i for one event m reads

$$S_{i,m}^{(r+1)} = M_W - \log A + \log A_0^{(r)}(R). \tag{5}$$

We allocate the station correction factor for the $(r+1)$th iteration as the sample mean of the station correction at different events. Assuming that there are a total of n events that station i records, the station correction estimation for the $(r+1)$th iteration reads

$$S_i^{(r+1)} = \frac{S_{i,1}^{(r+1)} + \cdots + S_{i,n}^{(r+1)}}{n} \tag{6}$$

Regression: This step corresponds to the M-step. Here, we use linear regression (least squares optimization) to obtain the model parameters, which is analogous to maximum likelihood estimation in the EM algorithm. Collecting the data pairs $(\log A_0, R)$ with the updated station corrections $S_i^{(r+1)}$, the updated $\log A_0$ reads

$$\log A_0 = \log A - M_W + S_i^{(r+1)}. \tag{7}$$

By assigning the updated $\log A_0$ as the response variable and the hypocentral distance R as the explanatory variable, we can derive a linear model via regression:

$$\log A_0(R) = A + B \cdot R + C \cdot \log R. \tag{8}$$

The result is the $(r+1)$th model $\log A_0^{(r+1)}(R)$. Note that in this project we use a more general linear model with three parameters.

After the convergence of both attenuation model coefficients and station corrections, we adopt the convention of setting the average station correction to zero. This step can be easily achieved by shifting the overall station corrections and corresponding A parameter in the attenuation model.

M_L estimation: By several iterations of alternating the E-step and M-step, the model parameters will converge. Convergence is the end of the EM algorithm, but one of our final goals is M_L estimation. Therefore, an extra step is required. Assuming that the station corrections converge to $\widehat{S_i}$ and the model of $\log A_0(R)$ converges to $\widehat{\log A_0(R)}$, M_L can be estimated as

$$\widehat{M_L} = \log A - \widehat{\log A_0(R)} + \widehat{S_i}. \tag{9}$$

Figure 1 shows the flowchart of the iterative regression. Given a $log A_0(R)$ model, the alternating estimation and regression will result in gradually improving both the station corrections and the model parameters. When both estimates converge, we use both the esimated $\widehat{\log A_0(R)}$ and $\widehat{S_i}$ to derive an accurate estimation of M_L. Note that in Eq. 9, both factors are estimated from the dataset. Thus, the issue of empirical station corrections assignment is resolved.

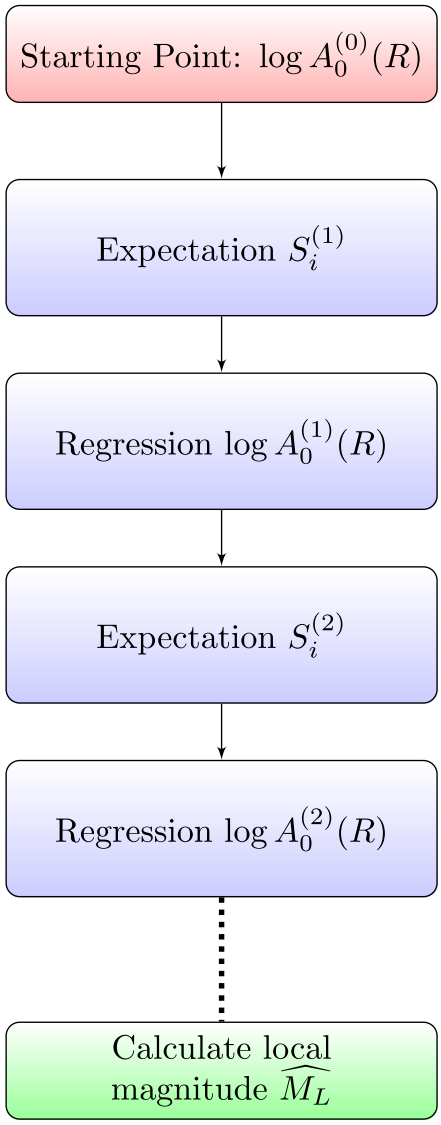

Fig. 1 Flowchart of the proposed iterative regression algorithm

4 Results

In the catalog dataset of Taiwan, there are two different types of acceleration amplitude records: a force-balance accelerometer (FBA) type and short-period velocity S-13 seismometer (S13) type. The FBA uses the relative displacement in a feedback loop to apply a current, while the S-13 is a passive seismometer, which does not have feedback current features (Collette et al. 2012). While most of the S13 type data are obtained from the S-13 seismometer, sometimes the Central Weather Bureau fills in the missing values with broadband data. The CWB deconvolves the instrumental response and then convolutes the Wood-Anderson response to simulate the output of the Wood-Anderson seismograph.

In theory, the Wood-Anderson seismograph amplitude from the two datasets should coincide, but some deviations were still observed. These deviations could be caused by the difference in the instruments. S13 is a high-gain instrument that focuses on less shaking, while the FBA is a low-gain instrument that can better record the larger shaking. The high-gain nature of the S13 sometimes causes saturation of the waveform; the CWB discards the data from S13 stations. Due to the

low-gain nature of the FBA, sometimes it does not register at the stations with less shaking. Therefore, the FBA dataset is not the same as the S13 dataset. Even considering the same event, at some stations, only the FBA registers, and vice versa. In addition to this difference, the mounting of the instrument can also affect the recorded waveform. FBAs are always mounted with an anchor, and S13s are often placed on a surface.

Due to the abovementioned instrumental difference, the FBA dataset and S13 dataset differ. We present the results of both datasets and compare them.

Figure 2 shows the convergence of the model statistics. The statistics include the residual standard error (RSE), R^2 and standard deviation of one station correction. We can observe that the fluctuation in the parameters converges after only a few iterations. We stopped the process at the fifth iteration because the updating values became trivial. Fast convergence was obtained because we employed the model from a previous study as the starting model. Since the previous model is passable, the final model is expected to strongly resemble the starting model.

The final model of the $\log A_0(R)$ reads

$$\begin{aligned}\log A_0(R) &= (-3.857 \times 10^{-1} \pm 3.722 \times 10^{-2}) \\ &\quad +(-2.646 \times 10^{-3} \pm 5.929 \times 10^{-5})R \\ &\quad +(-1.085 \pm 2.146 \times 10^{-2}) \log(R) \\ R^2 &= 0.788,\ \text{RSE} = 0.290, \quad \text{(FBA)} \end{aligned} \tag{10}$$

$$\begin{aligned}\log A_0(R) &= (-4.450 \times 10^{-1} \pm 6.157 \times 10^{-2}) \\ &\quad +(-3.041 \times 10^{-3} \pm 7.393 \times 10^{-5})R \\ &\quad +(-1.134 \pm 3.356 \times 10^{-2}) \log(R) \\ R^2 &= 0.753,\ \text{RSE} = 0.358, \quad \text{(S13)} \end{aligned} \tag{11}$$

Compared with the model from a previous study,

$$\log A_0(R) = 2.47 \times 10^{-1} – 2.81 \times 10^{-4} R – 1.509 \log(R). \tag{12}$$

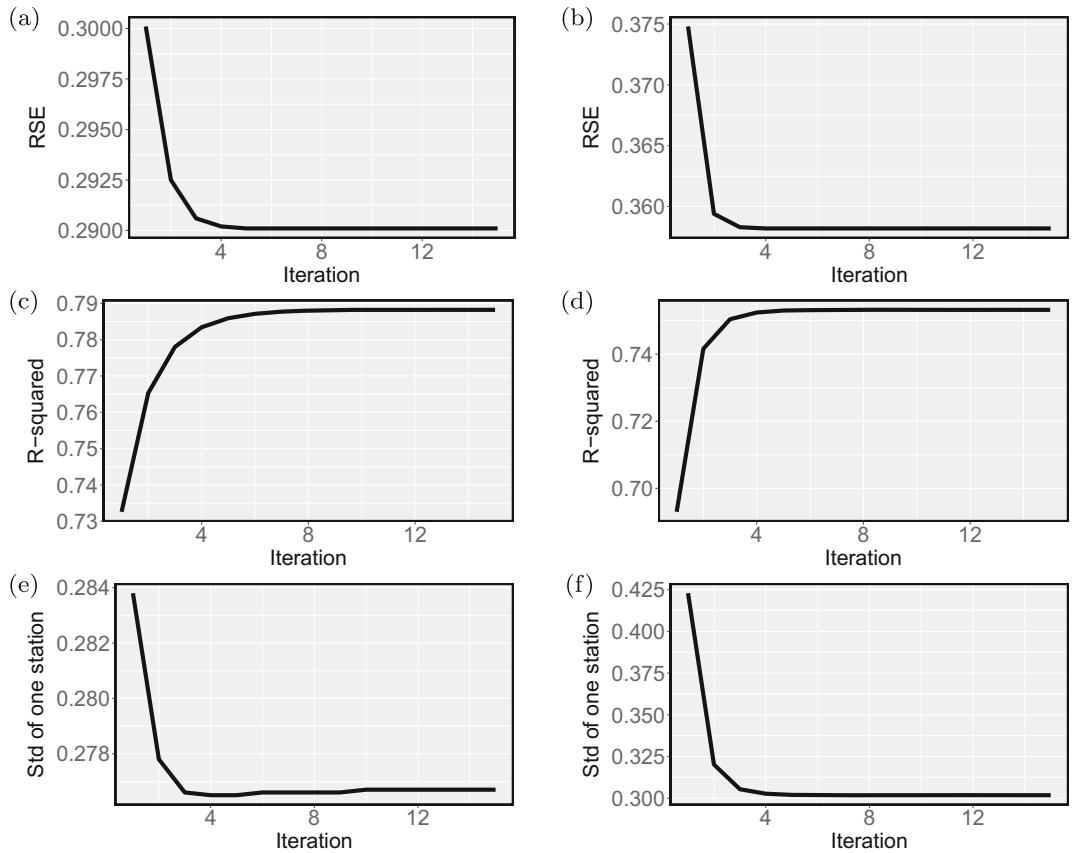

Fig. 2 Figures illustrating regression parameters versus iterations. The figures demonstrate the convergence achieved after several iterations. **a** RSE of FBA data. **b** RSE of S13 data. **c** R^2 of FBA data. **d** R^2 of S13 data. **e** Standard deviation of single-station correction of FBA data. **f** Standard deviation of single-station correction of S13 data

Although the signs of the coefficients are consistent and the major factor is still the $\log(R)$ term, the effect of the R term in our model substantially increases its importance. Between the two data types, the FBA outperforms S13 with a smaller RSE and higher R^2.

Figure 3 shows a comparison among the three attenuation models. The attenuation model of the FBA shares a tendency that is similar to the attenuation model of S13. At 100 km, the S13 model is close to the -3 mark, while the FBA model is similar to the model of the previous study.

Figure 4 shows the comparison between our estimated M_L and the CWB-provided M_L with respect to the moment magnitude M_W. Both M_L values outperform the CWB-provided M_L and pass the consistency check by fitting M_W. Additionally, the quantitative regression indicators demonstrate the same trend:

$$M_L = 1.026M_W - 0.196 \quad \text{(FBA)}$$
$$R^2 = 0.696,\ \text{RSE} = 0.275, \quad \text{(FBA)} \tag{13}$$
$$M_L = 0.982M_W - 0.088 \quad \text{(S13)}$$
$$R^2 = 0.644,\ \text{RSE} = 0.299, \quad \text{(S13)} \tag{14}$$
$$M_L = 0.937M_W - 0.398 \quad \text{(CWB)}$$
$$R^2 = 0.588,\ \text{RSE} = 0.322, \quad \text{(CWB)} \tag{15}$$

Figure 5 shows the statistics of station correction and the correlation between FBA data and S13 data.

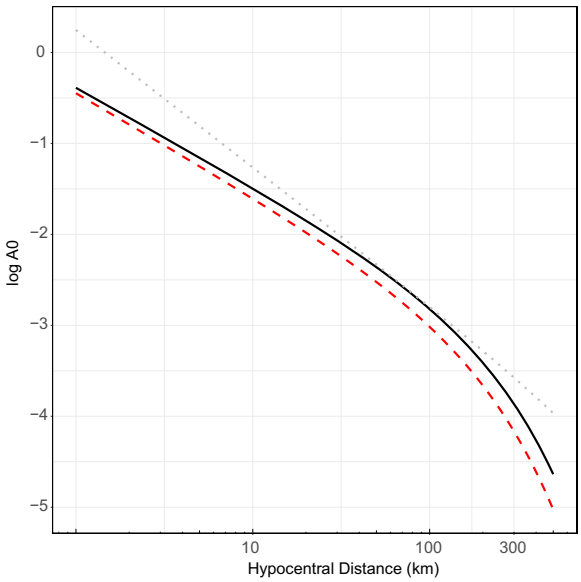

Fig. 3 Attenuation models. Solid line: FBA attenuation model. Dashed line: S13 attenuation model. Dotted line: attenuation model from Wu et al. (2005)

Subfigure (a) shows that the median FBA is closer to zero than the median S13. Subfigure (b) shows a high correlation of 0.864 between the two station corrections. In addition to the figure, we report the average standard deviation of station correction of FBA data type is 0.287, while the average standard deviation is 0.363 of S13 data type.

Figure 6 shows the spatial distribution of the station corrections of both types. Overall, the west side of Taiwan shows smaller station corrections than the east side for both types. This tendency is consistent with both the previous study (Wu et al. 2005) and the general geological setting of Taiwan, which is dominated by rock sites in the east and sedimentary sites in the west.

5 Discussion

5.1 Convergence property

Although the iterative regression method works very well with the given Taiwan dataset, the following question remains: do the results converge in other datasets or even with the same dataset with more entries in the future? The answer to this question is that the results will most likely converge under normality. To observe this convergence, we must consult the general convergence theorem of the EM algorithm (Dempster et al. 1977). The general theorem of EM guarantees that convergence is achieved and that the convergence parameters coincide with MLE without missing data. The basic notion of the statistics states that when least-squares optimization (regression) is performed with an error that is near the normal distribution, that is, $\epsilon \sim N(0, \sigma^2)$, the linear regression process is equivalent to the maximum likelihood function method with the bounded likelihood function, which is similar to the normal distribution MLE in the structure (correspondence between MLE and regression is recorded in many statistical treatises, for example, Hayashi (2011)). For a statistically meaningful regression, we already assume that the error satisfies a normal distribution. This normality makes the general convergence theorem applicable. Therefore, the iterative regression method converges if the mild condition of normality holds. If linear regression works, the iterative regression method will converge.

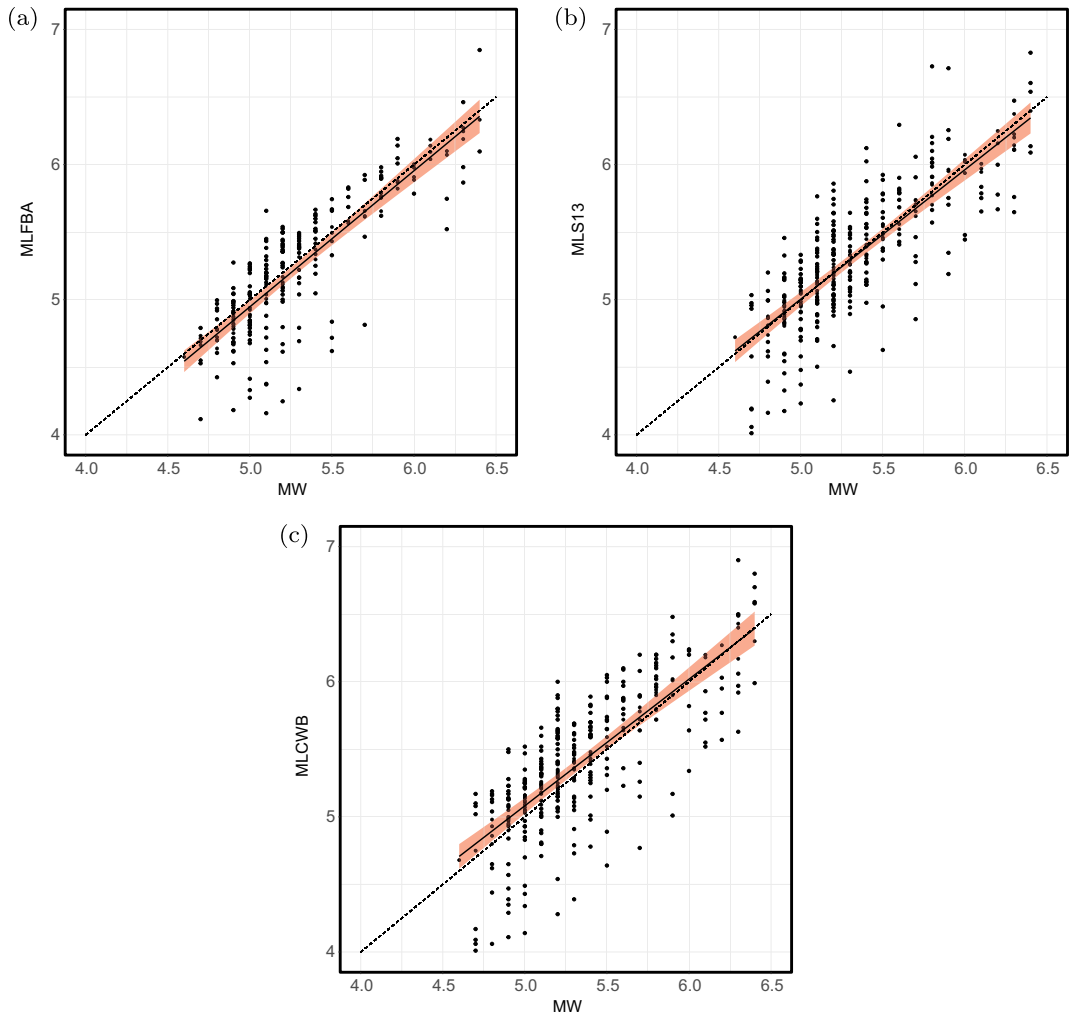

Fig. 4 Figures illustrating the linear relationship between M_L and M_W. **a** M_L of FBA vs M_W. **b** M_L of S13 vs M_W. **c** M_L of CWB vs M_W. The shaded areas correspond to the 99 percent confidence interval

5.2 General applicability

In some other regions that do not perform empirical station corrections, does the proposed method still apply? The answer is yes. Benefiting from the convergence property of the previously discussed iterative regression, the estimations are bound to converge to those of MLE, regardless of the starting model/starting values. Therefore, we can start the iteration by setting all station corrections to zero, $S_i^{(0)} = 0$. Based on this rough estimate, we can derive the primary linear model of the first iteration, that is, $\log A_0^{(1)}(R)$. The corresponding station corrections can be determined as $S_i^{(1)}$. Once the results of the first iteration are obtained, the next iteration can be calculated following the procedure of previous iterations. The only downside of a worse starting model is a possible longer computation time because it requires more iterations to achieve convergence.

5.3 Anchor point mismatch issue

The definition of the anchor point applied in the original M_L associates 100 km as -3. However, our models at 100 km deviate from this result (0.3 and 0.4). Superficially, the differences seem to

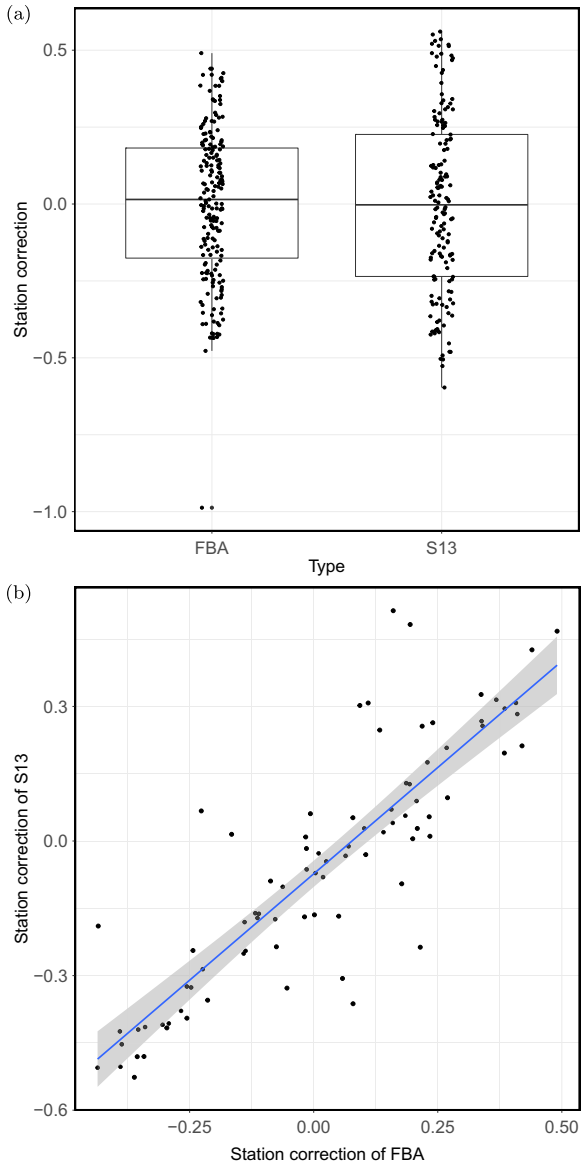

Fig. 5 Statistical distribution of station corrections and their correlation. **a** Boxplot of the two types of data. **b** Scatter plot of the two types of data

indicate an overall deviation in M_L, which is not valid. A major factor of these deviations is the extra effect from the station corrections. Considering the station at the anchor point, the original contribution of $-\log A_0(100)$ is +3. Moreover, the corresponding expression with the station correction reads $-\log A_0(100) + S_i$. An approximate estimation of the overall station correction around different stations gives $S = \mathbf{E}[S_i]$, where we use the expectation of the empirical distribution to account for the effect (essentially a weighted mean). The numerical results of the two data types give

$$-\log A_0(100) + S = 2.820 + 0.008 = 2.83 \quad \text{(FBA)} \tag{16}$$

$$-\log A_0(100) + S = 3.017 - 0.0237 = 2.993 \quad \text{(S13)}. \tag{17}$$

Note that after adding the expectation of station correction, both models are closer to anchor point 3. The remaining deviations are possibly attributable to the fluctuations in both the model and the station corrections. The paper (Shin 1993) utilized the S13 dataset and chose to use an anchor point of 100 km as −3 in Taiwan (compared to Southern California in the original definition). Comparing (Shin 1993) to our previously described results, the anchor point setting in Taiwan using S13 data seems to be a reasonable choice in hindsight.

5.4 Possible M_L/M_W scaling failure issue

Some previous studies indicate that for small-magnitude events, the ratio of M_L/M_W deviated from 1 to 1.5 (Hanks and Boore 1984; Bethmann et al. 2011). Deichmann (2017) further suggested that the ratio deviation is due to the attenuation effect that fixes the amplitude duration. Although similar observations were not found in Taiwan, some deviations are expected in the smaller events. The possible consequence of ratio deviation is that the matching procedure conducted in this study is affected and makes the smaller M_L less accurate. This finding constitutes a limitation of the proposed method in estimating smaller events.

5.5 Alternative approach

In statistics, the EM algorithm is not the only method that can account for missing data values. Another famous approach is Markov chain Monte Carlo (MCMC) analysis. This approach was originally developed to work with a strong correlation system with many molecules (Metropolis et al. 1953; Hastings 1970), where a deviation of position or interaction of one molecule affects all other molecules. Those effects are too large to use a perturbation approach. The idea of MCMC is to adjust pairs of molecules one

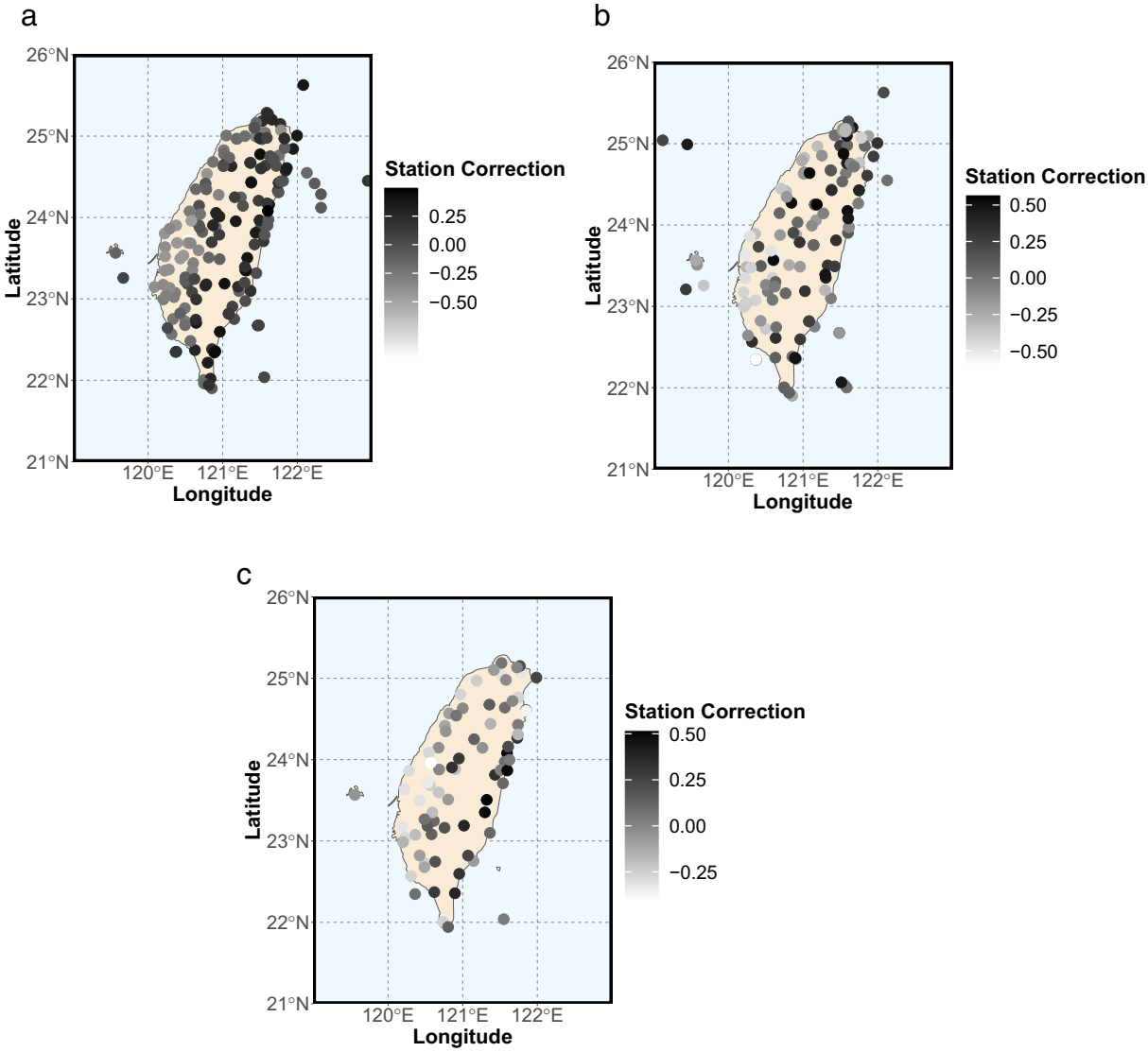

Fig. 6 Spatial distribution of station corrections. **a** FBA type. **b** S13 type. **c** Previous study (Wu et al. 2005)

at a time until thermal equilibrium is achieved. Many applications exist, in which the use of MCMC is significantly simpler than the EM algorithm approach. Takahashi (2017) surveyed the recent applications of MCMC for missing data. In this study, we did not choose the MCMC as our main approach because (1) the extra formalism employing MCMC is cumbersome and (2) the computational power required to carry out MCMC is greater than that of the proposed approach.

6 Conclusions

In this paper, we propose a new M_L method inspired by the EM algorithm to simultaneously estimate both the anchor attenuation linear model and station corrections.

As a numerical example, we use the proposed method to re-estimate M_L of Taiwan and find that the result achieves a better fit than the previous model. Additionally, the estimated station corrections show

a tendency that is similar to tendencies in previous studies and the geological setting in Taiwan.

In addition, we discuss the convergence property of the method and its general applicability. We expect the proposed method to routinely support future M_L and station correction estimation. Furthermore, the corresponding updated Taiwan M_L catalog is expected to provide better accuracy of the seismic release energy for future studies.

Acknowledgments Our work was supported by the Ministry of Science and Technology (MOST) of Taiwan under MOST 106-2116-M-002-019-MY3 and MOST 109-2116-M-002-030-MY3. Our work was also supported by the Research Center of Future Earth of the National Taiwan University under grant number 107L901002 and financially supported by the NTU Research Center for Future Earth from The Featured Areas Research Center Program within the framework of the Higher Education Sprout Project by the Ministry of Education (MOE) in Taiwan.

Author contribution T.C. H developed the theoretical formalism and wrote the paper. Y.M. W supervised the findings of this work. All authors discussed the results and contributed to the final manuscript.

Availability of data and materials Earthquake catalog data were obtained from the CWB in Taiwan (CWB website).

Declarations

Competing interests The authors declare no competing interests.

References

Bethmann F, Deichmann N, Mai PM (2011) Scaling relations of local magnitude versus moment magnitude for sequences of similar earthquakes in Switzerland. Bull Seism Soc Am 101(2):515–534. https://doi.org/10.1785/0120100179

Bormann P, Giacomo D (2010) The moment magnitude and the energy magnitude: common roots and differences. J Seismol 15(2):411–427. https://doi.org/10.1007/s10950-010-9219-2

Collette C, Janssens S, Fernandez-Carmona P, Artoos K, Guinchard M, Hauviller C, Preumont A (2012) Review: inertial sensors for low-frequency seismic vibration measurement. Bull Seism Soc Am 102(4):1289–1300. https://doi.org/10.1785/0120110223

Deichmann N (2017) Theoretical basis for the observed break in m_L/m_W scaling between small and large earthquakes. Bull Seism Soc Am 107(2):505–520. https://doi.org/10.1785/0120160318

Dempster AP, Laird NM, Rubin DB (1977) Maximum likelihood from incomplete data via the EM algorithm. J R Stat Soc B 39(1):1–38. https://doi.org/10.1111/j.2517-6161.1977.tb01600

Di Bona M (2016) A local magnitude scale for crustal earthquakes in Italy. Bull Seism Soc Am 106(1):242–258. https://doi.org/10.1785/0120150155

Hanks TC, Boore DM (1984) Moment-magnitude relations in theory and practice. J Geophys Res 89(B7):6229–6235. https://doi.org/10.1029/JB089iB07p06229

Hartley H (1958) Maximum likelihood estimation from incomplete data. Biometrica 14:174–194. https://doi.org/10.2307/2527783

Hastings WK (1970) Monte Carlo sampling methods using Markov chains and their applications. Biometrica 57:97–109. https://doi.org/10.2307/2334940

Hayashi F (2011) Econometrics. Princeton University Press, New Jersey

Kanamori H, Jennings PC (1978) Determination of local magnitude, m_L, from strong motion accelerograms. Bull Seism Soc Am 68(2):471–485

Kanamori H, Maechling HP, Hauksson E (1999) Continuous monitoring of ground-motion parameters. Bull Seism Soc Am 89(1):311–316

McLachlan GJ, Krishnan T (2008) The EM algorithm and Extensions, 2nd edn. Wiley-Interscience, Hoboken

Metropolis N, Rosenbluth AW, Rosenbluth MN, Teller AH, Teller E (1953) Equation of state calculations by fast computing machines. J Chem Phys 21:1087–1092. https://doi.org/10.1063/1.1699114

Neal RM, Hinton GE (1998) A view of the EM algorithm that justifies incremental, sparse, and other variants in Learning in Graphical Models: 355-368. Kluwer, Dordrecht

Rhoades DA, Christophersen A, Bourguignon S, Ristau J, Salichon J (2020) A depth-dependent local magnitude scale for New Zealand earthquakes consistent with moment magnitude. Bull Seism Soc Am:1–11. https://doi.org/10.1785/0120200252

Richter CF (1935) An instrumental earthquake scale. Bull Seism Soc Am 25(1):1–32. https://doi.org/10.1785/0120050043

Ristau J, Harte D, Salichon J (2016) A revised local magnitude (m_L) scale for New Zealand earthquake. Bull Seism Soc Am 106(2):398–407. https://doi.org/10.1785/0120150293

Shin TC (1993) The calculation of local magnitude from the simulated Wood-Anderson seismograms of the short-period seismograms. TAO 4:155–170. https://doi.org/10.3319/TAO.1993.4.2.155(T)

Takahashi M (2017) Statistical inference in missing data by MCMC and non-MCMC multiple imputation algorithms: assessing the effects of between-imputation iterations. Data Sci J 16(37):1–17. https://doi.org/10.5334/dsj-2017-037

Thurber C, Eberthart-Phillips D (1999) Local earthquake tomography with flexible gridding. Comp Geosci 25(7):809–818. https://doi.org/10.1016/S0098-3004(9907-2)

Wu YM, Chang CH, Hsiao NC, Wu FT (2003) Relocation of the 1998 Rueyli, Taiwan, earthquake sequence using three-dimensions velocity structure with stations corrections. TAO 14:421–430. https://doi.org/10.3319/TAO.2003.14.4.421(T)

Wu YM, Allen RM, Wu CF (2005) Revised m_L determination for crustal earthquakes in Taiwan. Bull Seism Soc Am 95(6):2517–2524. https://doi.org/10.1785/0120050043

Wu YM, Chang CH, Zhao L, Shyu JBH, Chen YG, Sieh K, Avouac JP (2007) Seismic tomography of Taiwan: improved constraints from a dense network of strong-motion stations. J Geophys Res 112(B08312):2517–2524. https://doi.org/10.1029/2007JB004983

Wu YM, Chang CH, Zhao L, Teng TL, Nakamura M (2008) A comprehensive relocation of earthquakes in Taiwan from 1991 to 2005. Bull Seism Soc Am 98(3):1471–1481. https://doi.org/10.1785/0120070166

Wu YM, Shyu JBH, Chang CH, Zhao L, Nakamura M, Hsu SK (2009) Improved seismic tomography offshore northeastern Taiwan: implications for subduction and collision processes between Taiwan and the southernmost Ryukyu. Geophys J Int 178:1042–1054. https://doi.org/10.1111/j.1365-246X.2009.04180.x